3

Optics of Astigmatism and Retinal Image Quality

M. Vilaseca, F. Díaz-Doutón, S. O. Luque,
M. Aldaba, M. Arjona and J. Pujol
Centre for Sensors, Instruments and Systems Development (CD6)
Universitat Politècnica de Catalunya (UPC)
Spain

1. Introduction

In the first part of this chapter, the optical condition of astigmatism is defined. The main causes and available classifications of ocular astigmatism are briefly described. The most relevant optical properties of image formation in an astigmatic eye are analysed and compared to that of an emmetropic eye and an eye with spherical ametropia. The spectacle prescription and axis notation for astigmatism are introduced, and the correction of astigmatism by means of lenses is briefly described.
The formation of the retinal image for extended objects and the related blurring are also analysed, and the real limits of tolerance of uncorrected astigmatism are provided. Simulations of retinal images in astigmatic eyes, obtained by means of commercial optical design software, are also presented.
Finally, the clinical assessment of retinal image quality by means of wavefront aberrometry and double-pass systems in eyes with astigmatism is presented, and current trends in research related to this topic are highlighted.

2. Optics of astigmatism

2.1 Definition, causes and classification

Astigmatism is a meridian-dependent type of refractive error that is present in most human eyes (Rabbets, 2007; Tunnacliffe, 2004; Atchison & Smith, 2000). Astigmatic (or toroidal) surfaces have two principal meridians, with the curvature of the surface ranging from a minimum on one of these meridians to a maximum on the other. Clinically, this refractive anomaly is described as a bivariate quantity consisting of an astigmatic modulus and axis (McKendrick & Brennan, 1996).
The main known causes of ocular astigmatism are hereditary and involve a lack of symmetry on the optical surfaces of the cornea and the crystalline lens. The main factors contributing to corneal and lenticular astigmatism are the following:

- Non-spherical surfaces (usually the front surface of the cornea).
- Tilting and/or decentring of the crystalline lens with respect to the cornea.

Other less frequent causes of astigmatism can also be cited: refractive index variation in some meridians of the eye due to a rare pathological condition; and irregular astigmatism,

which notably occurs in corneal conditions such as keratoconus, where the principal meridians are not perpendicular to each other.
Astigmatism can be classified according to several different factors:

- The associated spherical refractive errors:
  - Compound hypermetropic astigmatism, in which both principal meridians have insufficient refractive power for the length of the eye.
  - Simple hypermetropic astigmatism, in which only one principal meridian has insufficient refractive power for the length of the eye, while the other is emmetropic.
  - Mixed astigmatism, in which one principal meridian has insufficient refractive power for the length of the eye while the other has too much refractive power.
  - Simple myopic astigmatism, in which only one principal meridian has too much refractive power for the length of the eye, while the other is emmetropic.
  - Compound myopic astigmatism, in which both principal meridians have too much refractive power for the length of the eye.
- The axis direction:
  - With-the-rule astigmatism, in which the flattest meridian is nearer the horizontal than the vertical (90 ± 30^o).
  - Against-the-rule astigmatism, in which the flattest meridian is nearer the vertical than the horizontal (0 ± 30^o).
  - Oblique astigmatism, in which the principal meridians are more than 30^o from the horizontal and vertical meridians (45 ± 15^o).
- The regularity of surfaces:
  - Regular astigmatism, in which the principal meridians are perpendicular to each other and therefore correctable with conventional ophthalmic lenses.
  - Irregular astigmatism, in which the principal meridians are not perpendicular to each other or there are other rotational asymmetries that are not correctable with conventional ophthalmic lenses.

Many authors have measured the values and types of astigmatism exhibited by the human population (Baldwin & Mills, 1981; Kragha, 1986). There are various causes of change in eye astigmatism, including age and accommodation (Artal et al., 2002; Saunders, 1986, 1988; Atkinson, 1980; Gwiazda et al., 1984; Ukai & Ichihashi, 1991; Millodot & Thibault, 1985) and surgery (Bar-Sela et al., 2009; de Vries, 2009; Yao et al., 2006; Vilaseca et al., 2009a).

2.2 The retinal image of a point object

In an emmetropic eye or in an eye with spherical ametropia, rays diverging from a point on the axis are converged to a conjugate image point provided that the paraxial approximation is taken into account. In an eye with regular astigmatism, the image of a point object is not a point because of the different refractive powers corresponding to each of the principal meridians. In this case, the image of a point object is generally an ellipse, as shown in Figure 1.
The figure shows the main features of the refracted pencil in an astigmatic eye. For convenience, the principal meridians denoted as y and z are presented in the vertical and horizontal directions, respectively. In this particular case, the vertical meridian (y) has the greatest optical power and a focal line F'_y. This means that parallel rays contained in a vertical plane will be converged onto a point located on this focal line, while parallel rays

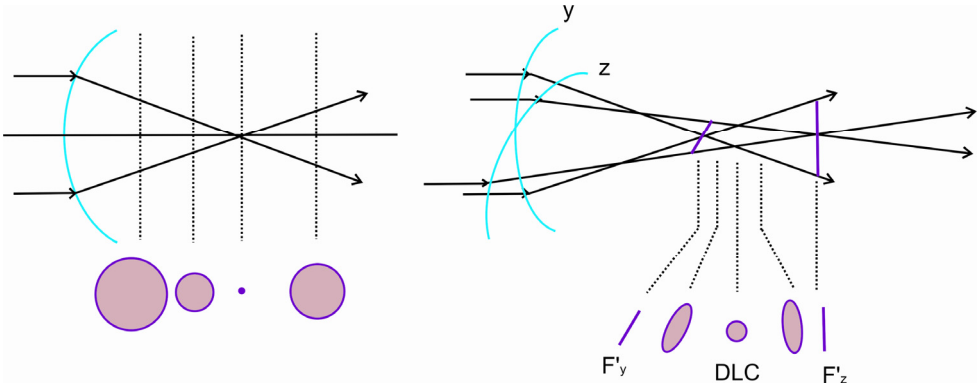

Fig. 1. Plots showing image formation in an emmetropic eye or an eye with spherical ametropia (left) and in an eye with a with-the-rule astigmatic refractive error (right). The principal meridians (y, z), the first and second focal lines (F'_y, F'_z), and the disc of least confusion (DLC) are shown.

contained in a horizontal plane will be converged onto a point located on the focal line F'_z. At any other distance other than that of the two focal lines, the cross-section of the refracted pencil is generally an ellipse. Precisely at the dioptric midpoint between the two focal lines, the cross-section of the pencil is circular and is called the disc of least confusion (DLC). The region between these two focal lines is known as the conoid of Sturm or Sturm's interval. The characteristics of the blurred ellipse depend on the pupil diameter and on the type of astigmatism (Charman & Voisin, 1993a, 1993b; Keating & Carroll, 1976).

2.3 Ocular refraction: notation and correction

Refraction (defined as the vergence of the eye's far point [or *punctum remotum*], i.e. the point conjugate with the fovea of the unaccommodated eye) is generally used to quantify any spherical or astigmatic ametropia. In the case of astigmatism (A), the absolute value of the difference between the refraction of the most powerful meridian (R_y) and that of the flattest one (R_z) is commonly used. This is equivalent to computing the difference in terms of refractive power between the least powerful meridian (P_z) and the most powerful one (P_y):

$$A = \left|R_y - R_z\right| = \left|P_z - P_y\right| \quad (1)$$

The notation commonly employed for astigmatism is the one also typically used for the prescription of sphero-cylindrical lenses. Astigmatism can therefore be thought of as being formed by the following components: sphere (S); cylinder (C), which describes how the most different meridian differs from the sphere; and axis (α) (Figure 2). In the notation for astigmatism, the refraction corresponding to the most powerful plane is often given first (R_y), followed by the value of the astigmatism (A), and finally the axis of the most powerful meridian (α_y) (see Equation 2). However, there is also another possibility: the refraction corresponding to the least powerful meridian can be given first (R_z), followed by the value of the astigmatism but with the sign changed (-A), and finally the axis of the least powerful meridian (α_z). These two options—the "plus cylinder notation" and the "minus cylinder

notation"—are the two conventions for indicating the amount of astigmatism in a spectacle prescription.

$$\begin{matrix} S & C & \alpha \\ R_y & A & \alpha_y \\ R_z & -A & \alpha_z \end{matrix} \quad (2)$$

The following is an example of spectacle prescription. Consider an eye with compound hypermetropic astigmatism with refractions of +1.00 D in the vertical meridian (R_{90^o} = +1.00 D) and +2.00 D in the horizontal meridian ($R_{0^o} = R_{180^o}$ = +2.00 D), that is, with-the-rule. Using Equation 1, the astigmatism of this eye can be quantified (A= $R_{90^o} - R_{0^o}$ = -1.00 D). Therefore, the notation of the astigmatism will be +2.00 -1.00 0^o (or equivalently 180^o) or +1.00 +1.00 90^o.

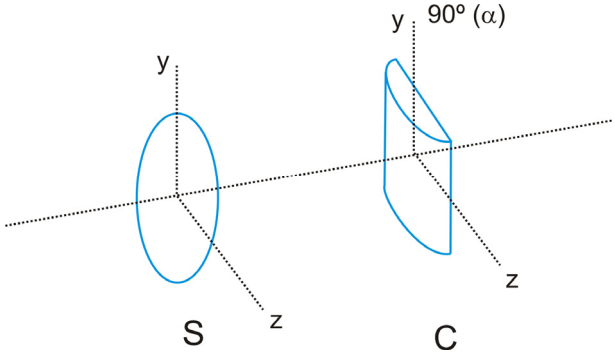

Fig. 2. Components of a sphero-cylindrical lens prescription (S: sphere, C: cylinder, α: axis)

From this analysis, it is clear that people with astigmatism have blurred vision at all distances, although this may be worse for distant or near vision, depending on the type of astigmatism. The most common way to correct astigmatism is by means of an astigmatic ophthalmic lens, although contact lenses and refractive surgery (laser corneal treatments and intraocular lens implants) are also available. In the astigmatic eye, the patient needs a different correction power for each principal meridian of the eye. Ophthalmic lenses for astigmatism correction usually have a spherical surface as well as a toroidal one that is generally located on the back surface of the lens, and, as mentioned above, are often called sphero-cylindrical lenses. For proper correction, the principal meridians of the lens must be aligned with those of the astigmatic eye, and the principal refractive powers must be such that each principal focus of the lens coincides with the eye's far point (Figure 3).

2.4 The retinal image of an extended object

The formation of the retinal image of an extended object can be thought of as being composed of images of many individual points, each giving rise to its own astigmatic pencil. As shown above, the intersection of an astigmatic refracted pencil with the retina may form an ellipse (with specific orientation and elongation), a circle, or a line.

Figure 4 shows some examples of images of extended objects as a function of the position of the retina. The most favourable orientation, in which blurring is least apparent, is always perpendicular to the most emmetropic meridian.

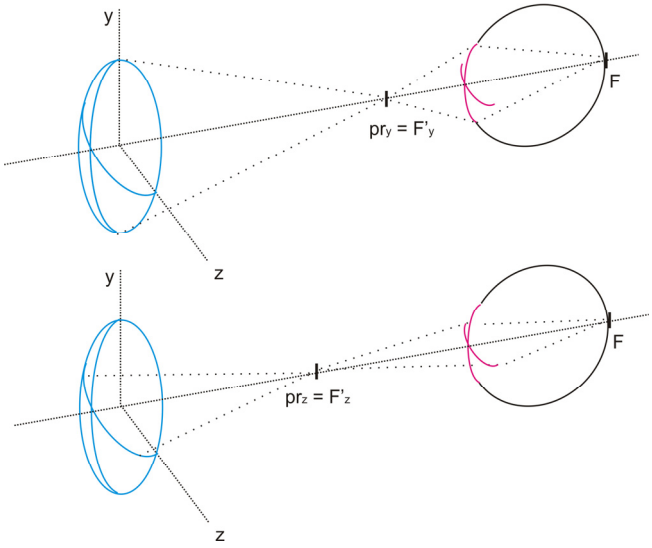

Fig. 3. In the correction of astigmatism by means of ophthalmic lenses, the principal meridians of the lens are aligned with those of the astigmatic eye (y, z), and the principal refractive powers are such that each principal focus of the lens (F'_y, F'_z) coincides with the eye's far point (pr_y, pr_z). The figure shows the correction of an eye with compound myopic astigmatism with the far point in front of each eye.

2.5 Simulations of the retinal image

The retinal image in an astigmatic eye can be simulated using commercially available optical design software. For most purposes, ocular astigmatism can be studied using schematic eyes, which have specific constructional data, Gaussian constants, cardinal points and aberrations (Atchison & Smith, 2000). From these elements, relevant information about the optical performance of the eye can be obtained. Moreover, software of this sort makes it possible to analyse the influence of several factors, such as pupil size and extra-axial field, on the retinal image. Theoretical models are now being widely used to gain more insight into the performance of various optical systems, such as contact and intraocular lenses, together with the eye.

For an eye with astigmatism of 1 DC (dioptres cylinder), Figure 5 shows simulations of images obtained at different planes using the OSLO® commercial software. Simulations were carried out with artificial eyes using a paraxial model (Le Grand eye model) and a finite model with aspherical surfaces (Navarro eye model) (Atchison & Smith, 2000; Navarro et al., 1985). A 4-mm pupil diameter and an angular field of 25° were considered.

3. Vision and tolerances to uncorrected astigmatism

3.1 Vision in uncorrected astigmatism

This section discusses vision in uncorrected astigmatism, taking into account the paraxial approximation. The size and blur of the retinal image for an uncorrected astigmatic eye are presented, taking into account the corresponding mean ocular refraction. These factors may have a relevant impact on current ophthalmologic practice.

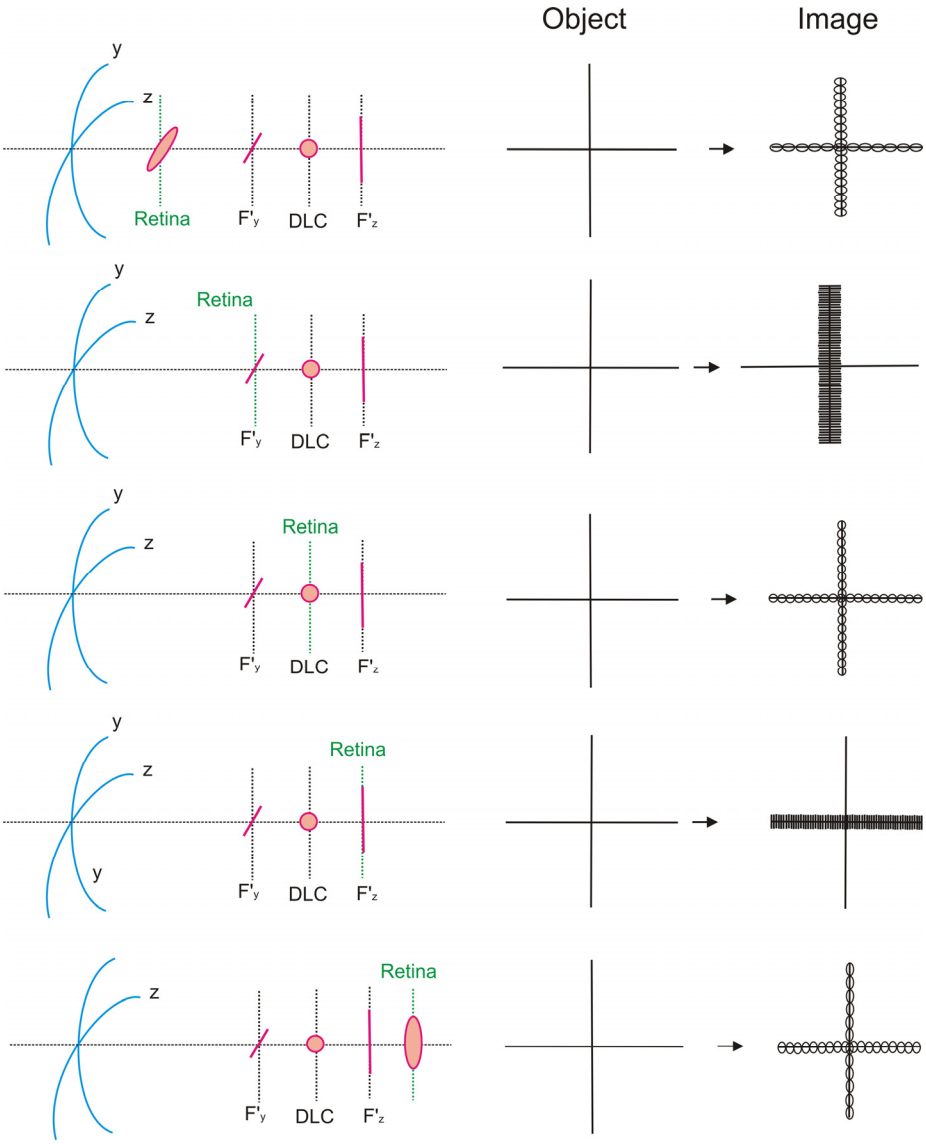

Fig. 4. Examples of image formation for extended objects as a function of the position of the retina (DLC: disc of least confusion; F'_y and F'_z: first and second focal lines).

Firstly, let us introduce the concept of mean ocular refraction (R_{mean}), also commonly known as spherical equivalent, which is the mean of the refractive errors in the two principal meridians of an astigmatic eye. The spherical equivalent gives the position of the DLC in terms of ametropia. Continuing with the example presented in a previous section, an eye with compound hypermetropic astigmatism of +2.00 -1.00 180º would have a mean ocular refraction of +1.50 D. In this example, it is likely that the patient can put the DLC, which is

the most favourable cross-section of the astigmatic pencil, into focus, provided that sufficient accommodation is available (i.e. the patient is healthy and young). Taking all this into account, the diameter of the DLC (ϕ_{DLC}) can be computed as a function of the astigmatism as follows:

$$\phi_{DLC} = \left| \phi_{PE} \cdot \frac{A}{2 \cdot (R_{\text{mean}} + P_{\text{mean}})} \right| \tag{3}$$

where ϕ_{PE} is the eye's entrance pupil diameter and P_{mean} is the average refractive power of the astigmatic eye, that is, $\frac{1}{2} \cdot \left(P_y + P_z \right)$.

As an example, Figure 6 shows the size of the DLC corresponding to eyes with uncorrected compound hypermetropic astigmatisms ranging from 0.25 to 3.00 DC. In accordance with the example given above (with-the-rule astigmatism), the following values are considered in the calculations: P_y = +59.00D (R_y = +1.00D, if the reduced eye model is considered) and $+56.00 \leq P_z \leq +58.75$ D.

If the DLC has been put into focus, the principal meridians of the astigmatic eye form the corresponding images of an extended object located at any distance in front of and behind the retina, respectively, thus obtaining a blurred retinal image. As stated above, this retinal image can be thought of as being composed of many DLCs, each corresponding to one point of the object, and the size of the blurred retinal image (y') can be calculated as follows (Figure 7):

$$y' = b + \phi_{DLC} = \left(\left| \frac{u}{R_y + P_y} \right| + \left| \phi_{PE} \cdot \frac{A}{2 \cdot (R_{\text{mean}} + P_{\text{mean}})} \right| \right) \tag{4}$$

where b is the size of the basic (sharp) retinal image that would be formed for a distant object subtending the same angle u.

The degree of blurring (DB) is then computed as the ratio between the diameter of the DLC and the size of the basic (sharp) retinal image as follows:

$$DB = \left| \frac{\phi_{DLC}}{b} \right| \tag{5}$$

Figure 8 shows two retinal images with different degrees of blurring but with basic (sharp) retinal images of the same size.

Figure 9 shows the degree of blurring corresponding to a far object (3 m) and a near object (40 cm) in eyes with uncorrected compound hypermetropic astigmatisms ranging from 0.25 to 3.00 DC.

In the case of an unaccommodated eye with spherical ametropia, the size of the DLC for a distant object can be computed as follows:

$$\phi_{DLC} = \left| \phi_{PE} \cdot \frac{R}{R + P} \right| \tag{6}$$

where R is the spherical refraction and P is the refractive power of the ametropic eye.

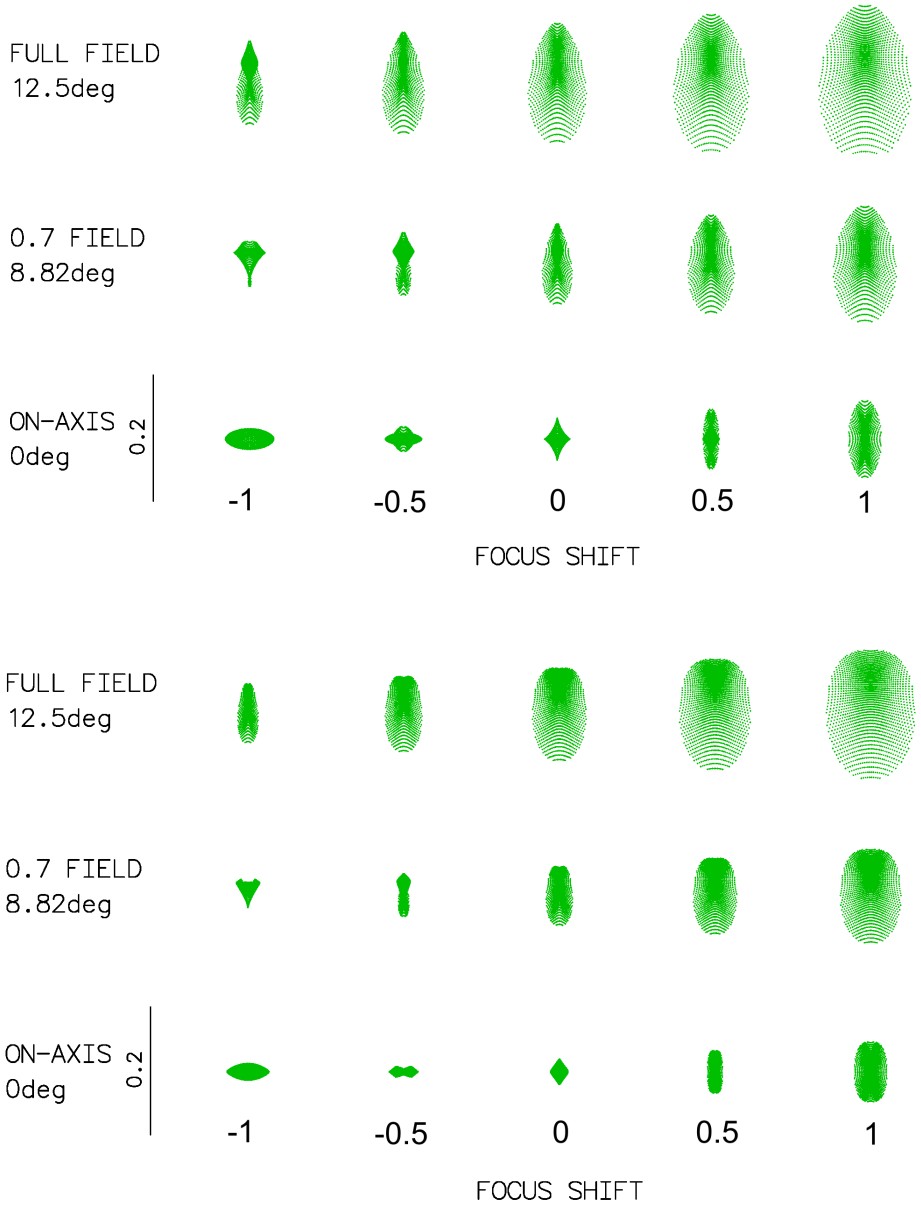

Fig. 5. Spot diagrams showing images at different planes corresponding to a point object of an eye with astigmatism of 1 DC, located on and off (8.82 and 12.5 degrees) the optical axis, simulated using the Le Grand artificial eye model (top) and the Navarro artificial eye model (bottom). A pupil diameter of 4 mm and an angular field of 25º were considered. Spot size is in millimetres and focus shift is in dioptres.

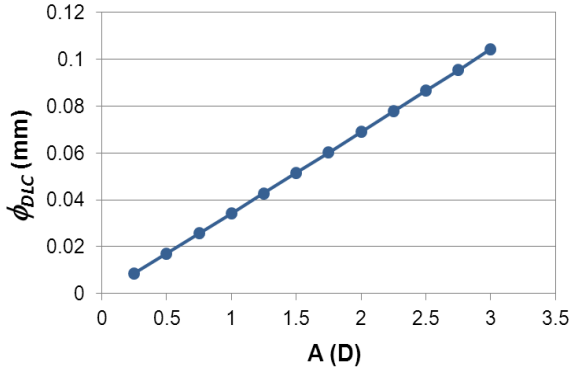

Fig. 6. Diameter of the disc of least confusion (ϕ_{DLC}) as a function of the astigmatism (A) (D: dioptres).

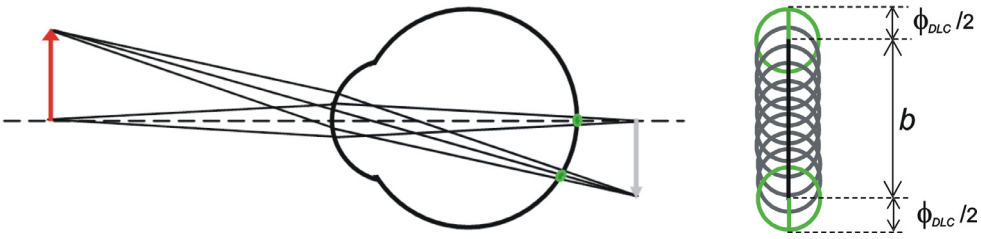

Fig. 7. Formation of the image of an extended object located at any distance for an eye with compound hypermetropic astigmatism; for convenience, only the image corresponding to the vertical meridian, located behind the retina, is shown (b: size of the basic [sharp] retinal image that would be formed for a distant object subtending the same angle u; ϕ_{DLC}: diameter of the disc of least confusion).

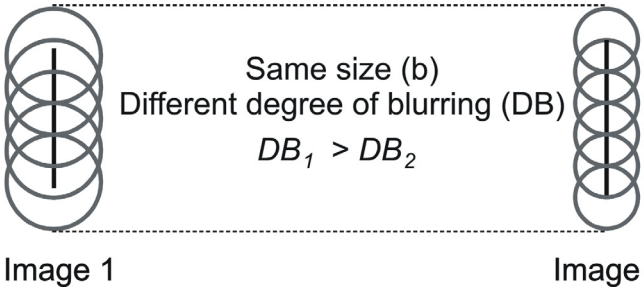

Fig. 8. Two examples of retinal images having basic (sharp) retinal images of the same size (b) but different degrees of blurring (DB) due to the different sizes of the discs of least confusion.

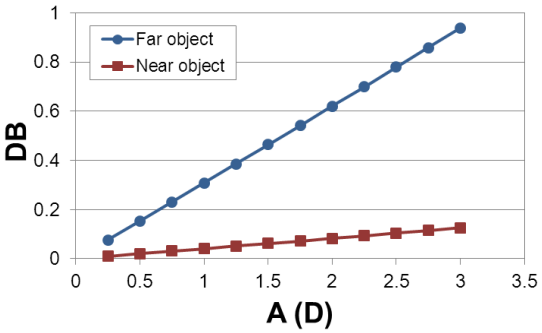

Fig. 9. Degree of blurring (DB) for far (3 m) and near (40 cm) objects as a function of the astigmatism (A) (D: dioptres).

Equations 3 and 6 show that, for a given entrance pupil size, the size of the DLC corresponding to a certain amount of astigmatism is only approximately half the size of the DLC generated by the same amount of spherical ametropia. Therefore, patients with astigmatism and the DLC focused on the retina theoretically have better vision than those with the same amount of spherical ametropia. This paraxial approximation supports the fact that a visual acuity of 6/18 was traditionally thought to indicate spherical ametropia of about 1.00 D or astigmatism of approximately 2.00 DC, provided that the DLC is focused on the retina (Rabbets, 2007). However, Section 3.3 will show that when all aberrations of the eye are considered—rather than the paraxial approximation—the difference in vision between spherical ametropia and astigmatism of the same amount is in fact much lower.
Finally, in eyes with myopic astigmatism, far vision cannot be improved by accommodation, so the patient would be expected to have vision similar to that of an eye with spherical ametropia equal to the corresponding spherical equivalent.

3.2 Lens rotation and mismatches in the cylinder

This section analyses the effects of lens rotation or mismatches in the cylindrical power of the lens used to correct astigmatism. It should be noted that the rotation of a cylindrical lens with respect to the eye results in a residual refraction consisting of a cylinder (C) and a sphere (S) due to the combination of two obliquely crossed cylinders.
In general, when two toroidal surfaces (with cylindrical powers of C_1 and C_2) are combined, they result in a residual error, which consists of the following components expressed in terms of sphero-cylindrical lens notation (Rabbets, 2007; Harris, 1988):

$$\begin{aligned} C &= \pm\sqrt{(C_1+C_2)^2 - 4C_1C_2\sin^2\alpha} \\ S &= \tfrac{1}{2}(C_1+C_2-C) \\ \theta &= \arctan\left(\frac{-C_1+C_2+C}{C_1+C_2+C}\right)\cdot\tan\alpha \end{aligned} \tag{7}$$

where α is the angle between cylindrical powers C_1 and C_2, and θ is the angle measured from C_1 to C (see Figure 10).

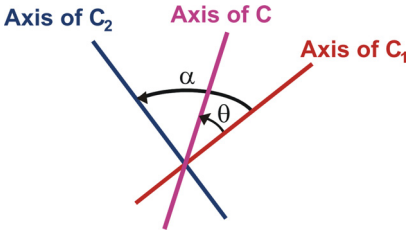

Fig. 10. Composition of two obliquely crossed cylinders with cylindrical powers of C_1 and C_2 (C: resultant cylinder).

Figure 11 shows an example of residual refraction in terms of cylinder and sphere as a function of the rotation angle, when the ophthalmic lens and the astigmatism of the eye have the same cylindrical powers and when they differ by 0.50 DC. Results are given for eyes with astigmatisms of 1 and 3 D, respectively.

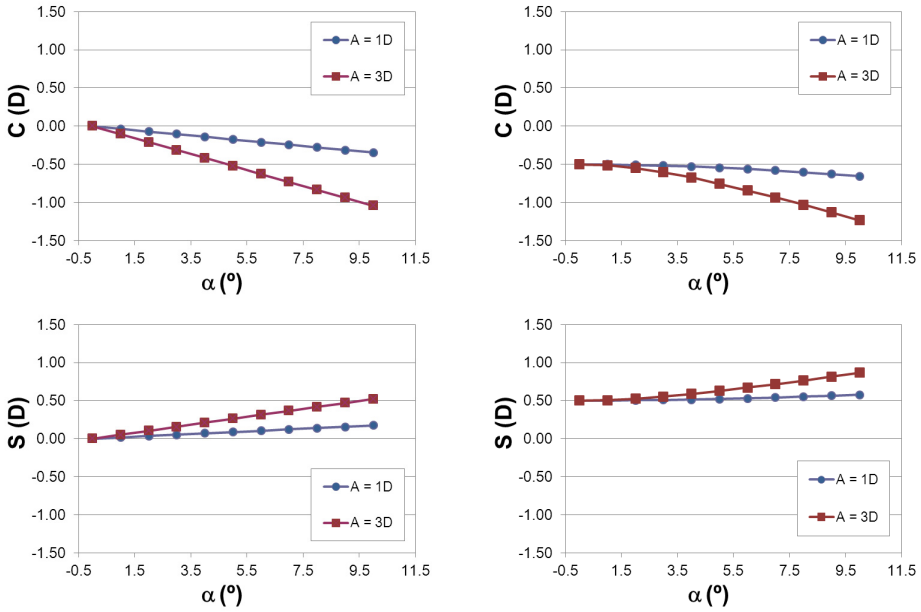

Fig. 11. Residual refraction as a function of the rotation angle between the cylindrical lens and the astigmatism axis (α) when the cylindrical power of the lens and the astigmatism of the eye have the same value (left) and when the cylindrical power of the lens and the astigmatism of the eye differ by 0.50 DC (right). Results are given for astigmatic eyes with cylinders of 1 and 3 DC, respectively (C: cylinder; S: sphere; D: dioptres; °: degrees).

3.3 Tolerances to uncorrected astigmatism

The question of the extent to which the retinal image may be degraded by defocus or astigmatism before it starts to be noticeably blurred has already been analysed taking into account the paraxial approximation. This question may play an important role in corrective

lens design and refractive surgery outcomes, among other issues. Some studies including experiments involving just-noticeable decreases in image clarity have suggested that the limits for astigmatism are about 1.4 times greater than those for defocus blur (0.32 DC as compared to 0.23 D) (Burton & Haig, 1984; Haig & Burton, 1987). Using a similar approach, Legras et al. found that the cross-cylinder blur limit was about 1.25 times higher than that found for defocus (Legras et al., 2004).

Sloan (1951) determined the relative effects of spherical and cylindrical errors on visual acuity and found that cylindrical errors reduce visual acuity at 0.8 the rate of spherical errors, while Raasch (1995) found that pure cylindrical errors reduced visual acuity at about 0.7 the rate of spherical errors. By carrying out visual acuity simulations, other authors have found that aberrations with low orientation dependence had greater effects than those with higher orientation dependence. In dioptric terms, the ratios of visual acuity loss with astigmatism as compared to defocus were 1.1 and 0.8 for high- and low-contrast letters, respectively (Applegate et al., 2003).

By using an experimental setup based on adaptive optics, Atchison et al. (2009) determined the level of additional aberration at which an individual with normal inherent levels of higher-order ocular aberration becomes aware of blur due to extra defocus or cross-cylinder astigmatism. Cross-cylinder astigmatic blur limits were found to be approximately 90% of those for defocus.

Charman & Voisin (1993b) approached the question of visual tolerance to uncorrected astigmatism by exploring the changes in the modulation transfer function (MTF), which represents the loss of contrast produced by the eye's optics as a function of spatial frequency. The authors found a reduction in the MTF and orientation dependence with the magnitude of the astigmatism. These effects tended to increase with the spatial frequency, but also with the pupil diameter and inversely with the wavelength, because all of these parameters affected the wavefront aberration. Tolerance to astigmatism deduced from purely optical considerations (based on the analysis of the wavefront aberration or changes in the ocular MTF) was found to be approximately 0.25 DC. Nevertheless, tolerance to refractive error depends upon both the changes in the optical image on the retina and the ability of the neural stages of the visual system to detect those changes. Some authors have suggested that, since in real life the peak of the neural contrast sensitivity function at spatial frequencies is lower than 10 cycles per degree (Campbell, 1965), the contrast of natural scenes is low, and the roll-off in the amplitude spectrum is approximately reciprocal to the spatial frequency (Tolhurst et al., 1992), visual tolerances to astigmatic error are more heavily weighted toward the lower end of the spatial frequency spectrum, which is less influenced by astigmatic errors. Hence, although the optical deficits of 0.50 and 0.75 DC appear substantial, some authors have argued that they might be well tolerated in everyday use by less critical observers, although visual discomfort might arise during more exacting tasks such as work at visual display terminals (Wiggins & Daum, 1991).

Although the paraxial approximation is a very useful tool for easily analysing the visual implications of spherical ametropia and astigmatism, the aforementioned results show that this optical approach may be misleading in analysing real tolerances to uncorrected astigmatism in the aberrated human eye (see Section 3.1). The experimental results described above support the notion that the vision differences reported between spherical and astigmatic refractive errors are considerably smaller than those suggested by the paraxial approximation.

4. Clinical assessment of retinal image quality in eyes with astigmatism

Retinal image quality can be clinically analysed using several different tools, such as wavefront aberrometers and double-pass systems. From them, relevant information on the optical quality of the retinal image, in particular of an eye with astigmatism, can be obtained.

Over the past decade, wavefront aberrometers have been widely used to determine retinal image quality in connection with customized wavefront-guided LASIK (Schallhorn et al., 2008; Dougherty & Bains, 2008). Most of these instruments are based on the Hartmann-Shack sensor (Prieto et al., 2000; Liang et al., 1994). They generally consist of a microlens array conjugated with the eye's pupil and a camera placed at its focal plane. If a plane wavefront reaches the microlens array, the image recorded with the camera is a perfectly regular mosaic of spots. If a distorted (that is, aberrated) wavefront reaches the sensor, the pattern of spots is irregular. From the displacement of the spots, the wavefront aberration can be computed by fitting to the Zernike polynomials and the MTF can also be calculated.

Some studies have analysed the wavefront aberrations of the eye as a function of age. Measurements of the total aberrations of the eye and of the aberrations of the anterior corneal surface suggest that astigmatism of the cornea is more widespread than astigmatism of the full eye in younger subjects (Artal et al., 2002). Other recent studies have focused on changes in refraction and peripheral aberrations as a function of accommodation (Mathur et al., 2009; Radhakrishnan & Charman, 2007). The authors of these studies generally found a small change in the astigmatic components of refraction or the higher-order Zernike coefficients, apart from fourth-order spherical aberration, which became more negative at all field locations. Researchers have recently demonstrated that certain combinations of non-rotationally symmetric aberrations, such as coma and astigmatism, can result in better retinal image quality as compared to the condition with the same amount of astigmatism alone (de Gracia et al., 2010). Other authors have studied the effect of cataract surgery on the optical aberrations of the eye, and astigmatism in particular (Montés-Micó et al., 2008; Guirao et al. 2004; Marcos et al., 2007). Most of these studies found that astigmatism increased significantly after surgery.

The double-pass technique has also been shown to be a useful tool for comprehensively evaluating retinal image quality in eyes affected by several optical conditions, such as defocus, astigmatism and higher-order aberrations. Double-pass systems are based on recording images from a point-source object after reflection on the retina and a double pass through the ocular media. Figure 12 shows a conventional layout of a double-pass system, which consists of a laser coupled to an optical fibre as a light source (LD). A motorized optometer consisting of two lenses (L3, L4) with a focal length of 100 mm and two mirrors (M2, M3) is used to measure the subject's defocus correction. A video camera (CCD1) records the double-pass images after the light is reflected on the retina and on a beam splitter (BS2). Pupil alignment is controlled with an additional camera (CCD2). A fixation test (FT) helps the subject during the measurements. The instrument has an artificial and variable exit pupil (ExP), controlled by a diaphragm wheel, whose image is formed on the subject's natural pupil plane.

Unlike standard wavefront aberrometry, double-pass systems directly compute the MTF from the acquired double-pass retinal image by Fourier transform, making possible the complete characterization of the optical quality of the eye (Santamaría et al., 1987). Because of the differences between the two technologies, recent studies have suggested that

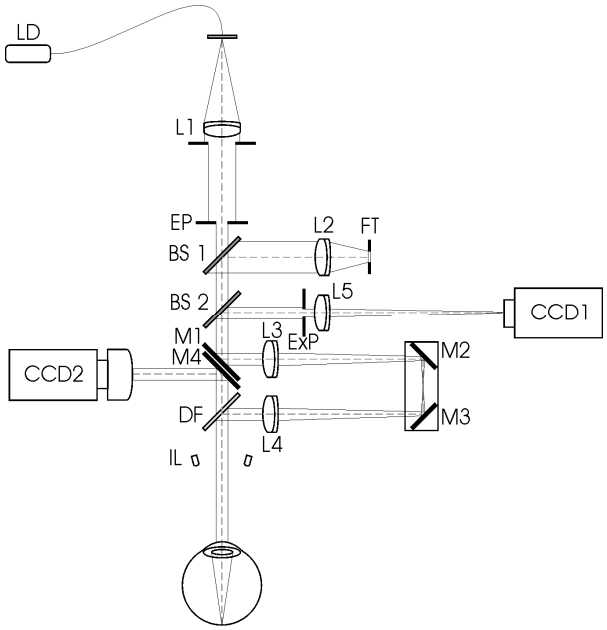

Fig. 12. Double-pass experimental setup (LD: laser; L1-L5: lenses; EP: entrance pupil; ExP: exit pupil; BS1, BS2: beam splitters; FT: fixation test; CCD1, CCD2: CCD cameras; M1-M4: mirrors; DF: dichroic filter; IL: infrared LED).

wavefront aberrometers may overestimate retinal image quality in eyes where higher-order aberrations and intraocular scattered light are prominent (Díaz-Doutón et al., 2006).

Figure 13 shows the double-pass images and the corresponding intensity profiles as a function of the angle (averaged section of the double-pass image), MTFs, and simulated vision using a standard visual acuity chart for an emmetropic eye, an eye with uncorrected astigmatism and an eye with spherical ametropia. The measurements were taken with the Optical Quality Analysis System (OQAS, Visiometrics, S.L., Spain) (Güell et al., 2006; Saad et al., 2010; Vilaseca et al., 2010a), which is a double-pass system currently available for use in daily clinical practice that includes this application.

The double-pass technique has been used extensively to determine the optical quality of the eye, mainly by means of the ocular MTF. Studies have revealed the potential of this technique in basic research (Artal et al., 1995a; Williams et al., 1994, 1996) and in its application to ophthalmology, optometry, and ophthalmic optics testing. In particular, it has been used to assess retinal image quality in patients with keratitis (Jiménez et al., 2009) and patients undergoing refractive surgery, such as LASIK (Vilaseca et al., 2009a; Vilaseca et al., 2010b) and intraocular lens implants (Vilaseca et al., 2009a; Alió et al., 2005; Fernández-Vega et al., 2009; Artal et al., 1995b). This technique has also been used to evaluate presbyopia after photorefractive keratectomy (Artola et al., 2006), to study retinal image quality in contact lens wearers (Torrents at al., 1997), and to analyse in vitro optical quality of foldable monofocal intraocular lenses (Vilaseca et al., 2009b).

Pujol et al. (1998) used the double-pass technique to study retinal image quality in eyes with uncorrected astigmatism. Performing direct optical measurements to characterize retinal

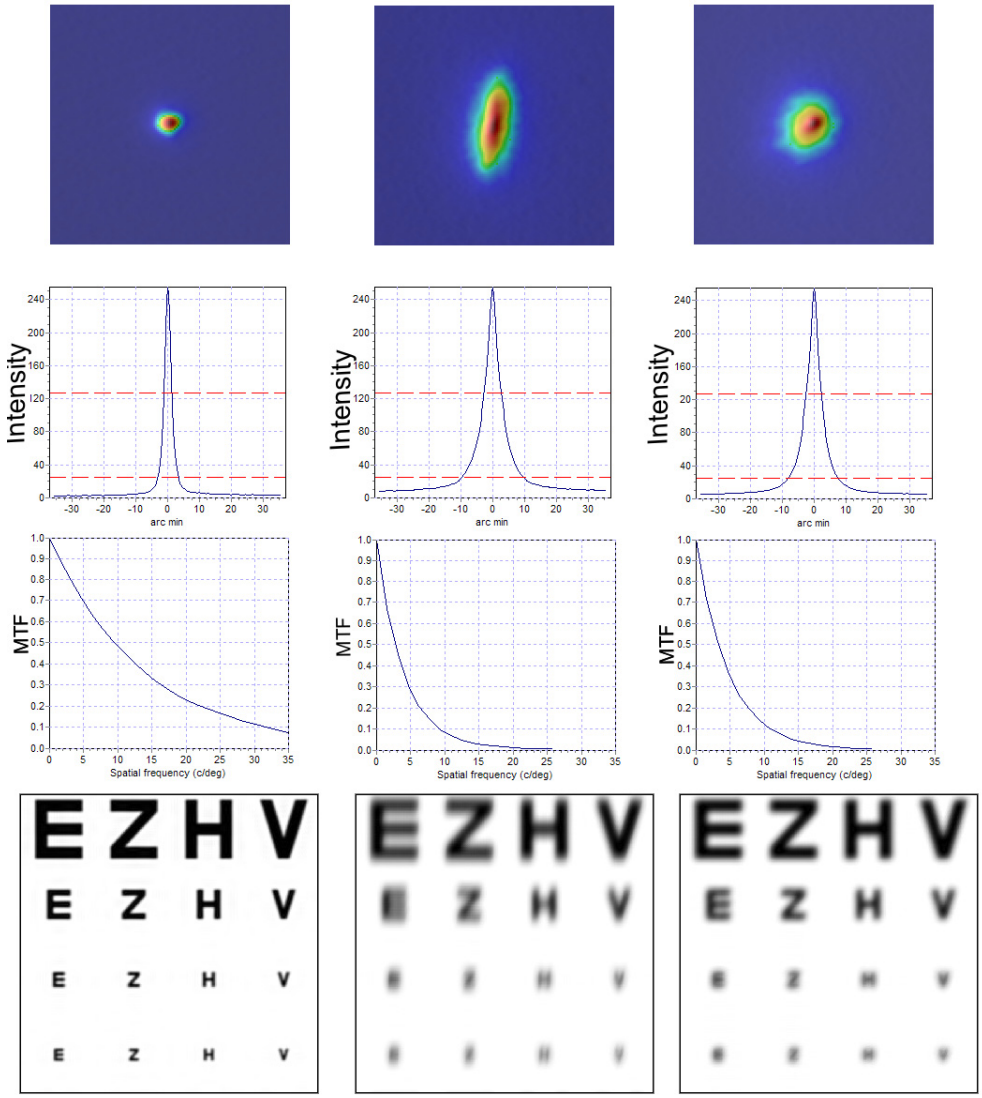

Fig. 13. Double-pass images corresponding to an emmetropic eye (left), an astigmatic eye (middle) and an eye with spherical ametropia (right). The corresponding intensity profiles as a function of the angle (minutes of arc [arc min]), MTF curves and simulated vision using a standard visual acuity chart are also provided.

image quality in astigmatic eyes can be advantageous since the standard clinical evaluation using visual acuity tests may be affected by non-optical problems in the subjects' visual system that cannot be separated from the optical ones. Pujol et al. studied the influence of the amount of astigmatism and changes in axis of astigmatism on the eye's optical

performance by means of numerical simulation using an emmetropic eye model (Navarro et al., 1985), an artificial eye, and three real subjects (JG, JP, VB) for a 4-mm artificial pupil. Different amounts of astigmatism were obtained by varying the cylindrical power of a lens situated in front of the eye, from 0.25 DC overcorrection to 1 DC undercorrection at intervals of 0.25 DC. Changes in the axis of astigmatism were obtained by rotating the lens, which neutralized the astigmatism in an angle of ±10° at 5° intervals.

The results showed a decrease in retinal image quality and an increase in the degree of image astigmatism as the amount of astigmatism increased (Figure 14) or when the angle between the lens and the eye axis was other than zero. In general, the largest variations were found when the astigmatism changed from 0 to 0.25 DC or when the axis changed from 0° to ±5°. Astigmatism reduced optical performance in the eye model, the artificial eye, and the living eyes, but in different proportions. The images obtained by simulation had better optical quality than those of the artificial eye, probably because exact focusing of the image was more difficult for the artificial eye than for the simulated eye. When these images were compared with those for the living eyes, considerable differences in shape and size due to the eye's optical performance were observed. The aberrations and intraocular scattering in living eyes introduced an additional blur into the retinal image that tended to reduce the loss of retinal image quality introduced by astigmatism.

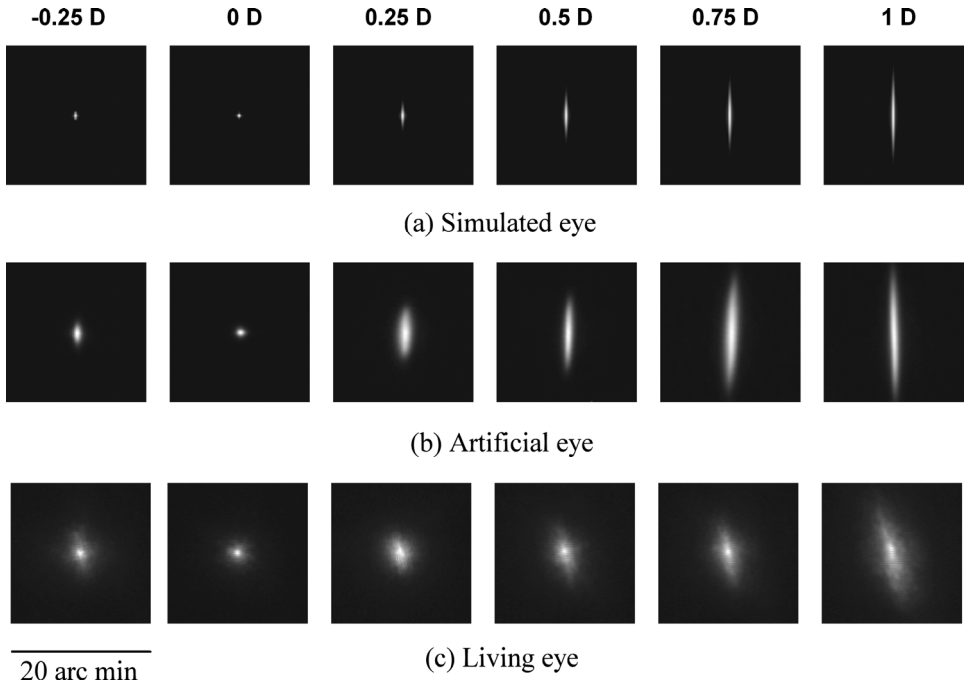

Fig. 14. Double-pass images numerically simulated in an eye model (a), measured in an artificial eye (b) and measured in a living eye (c) for different amounts of astigmatism. Negative values of astigmatism mean overcorrection and positive values mean undercorrection (source: Pujol et al., 1998).

The study also reported a reduction in the MTF with the presence of astigmatism. Figure 15 shows the MTF profiles in the direction of the low-power (solid curve) and high-power (dotted curve) principal meridians corresponding to the three subjects when astigmatism was 0 and 1 DC. Measurements were taken in the plane of the focal line corresponding to the low-power meridian. These profiles showed the minimum and maximum effects of

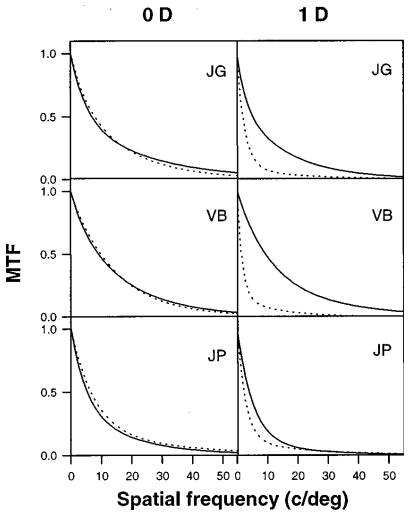

Fig. 15. MTF profiles in the direction of the low-power (solid curve) and the high-power (dotted curve) principal meridians for the three subjects and for astigmatisms of 0 and 1 DC (source: Pujol et al., 1998).

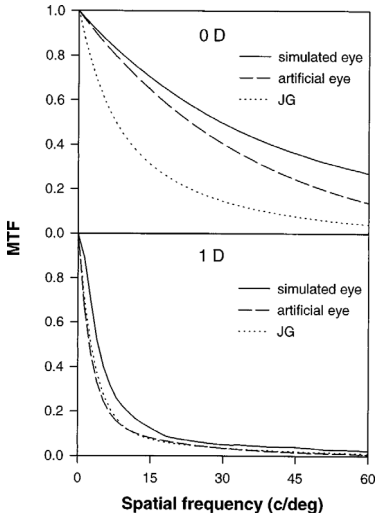

Fig. 16. Average MTF profiles for a simulated eye, an artificial eye, and a living eye (subject JG) at astigmatism values of 0 and 1 DC (source: Pujol et al., 1998).

astigmatism: the lower curve corresponds to the orientation showing the maximum elongation of the double-pass image, while the upper curve corresponds to the minimum elongation. In this context, Figure 16 shows the mean MTF obtained by averaging this function over all orientations for the simulated eye, the artificial eye, and the living eye (subject JG) when the astigmatism was 0 and 1 DC. For astigmatism of 0 DC, the highest optical performance was obtained for the eye model and the lowest for the living eye, which means that, when there is no dioptric blur in the retinal image, the aberrations present in the living eye are greater than those in the eye model. The optical performances of the living, artificial and simulated eyes were more similar for astigmatism of 1 DC than for 0 DC. At 0 DC, the associated dioptric blur was the greatest aberration.

Table 1. Refractive State of the Three Subjects Studied

Subject	Spherical Ametropia	Total Astigmatism
JG	−2.75 D	−1.00 D × 10°
VB	+0.25 D	−0.25 D × 0°
JP	+0.75 D	−0.75 D × 100°

Table 2. Residual Spherical–Cylindrical Power Obtained When the Axis of a Lens Correcting the Astigmatism of an Eye Formed Different Angles with the Axis of the Astigmatic Eye[a]

Subject	θ	S	C	α
VB	10°	0.04 D	−0.09 D	140°
	5°	0.02 D	−0.04 D	137.5°
	−5°	0.02 D	−0.04 D	42.5°
	−10°	0.04 D	−0.09 D	40°
JP	10°	0.13 D	−0.26 D	60°
	5°	0.06 D	−0.13 D	57.5°
	−5°	0.06 D	−0.13 D	142.5°
	−10°	0.13 D	−0.26 D	140°
JG	10°	0.17 D	−0.35 D	150°
	5°	0.09 D	−0.17 D	147.5°
	−5°	0.09 D	−0.17 D	52.5°
	−10°	0.17 D	−0.35 D	50°

[a] Results are shown for the three subjects who took part in the experiment. θ is the angle formed by the lens and the eye axis, S is the residual spherical power, C is the residual cylindrical power, and α is the axis of the residual refractive error.

Fig. 17. Refractive error of the three subjects (Table 1) and residual sphero-cylindrical power when the lens and eye axes are different (Table 2) (source: Pujol et al., 1998).

To evaluate the influence of variation in the axis of astigmatism on retinal image quality, the authors placed in front of the eye a lens whose cylindrical power was suitable for correcting the astigmatism and whose axis formed a particular angle with the axis of the astigmatic eye. This situation can occur in clinical practice when the correction axis and the eye axis are not coincident. Figure 17 shows the refractive errors and the residual sphero-cylindrical power for the three subjects and for the values of the angle formed by the lens and eye axes. According to Table 2, the retinal image quality decreased as the angular change in axis of astigmatism increased. For a particular angular value, the greatest variation was expected for subjects with a higher residual refractive error (JP, JG). However, the results did not show the proportional dependence on the residual refractive error that had been expected on the basis of the geometrical approximation. Again in this case, the aberrations (besides astigmatism) present in the living eye reduced the contribution of the residual sphero-cylindrical power to a decrease in retinal image quality.

Torrents et al. published a study in which they applied the double-pass technique to determine optical image quality in monofocal contact lens wearers and showed the

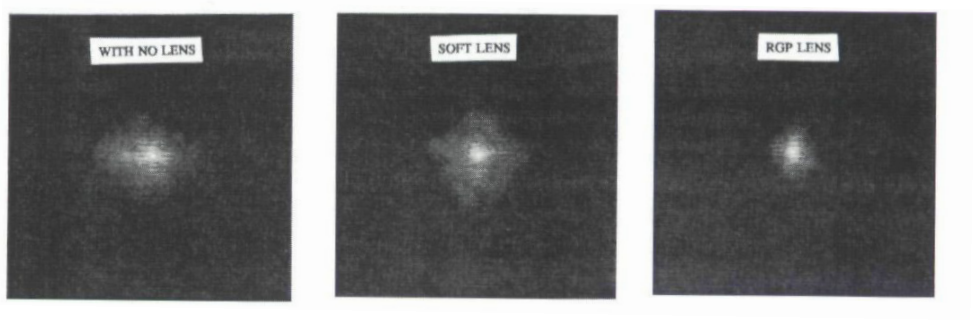

(a)

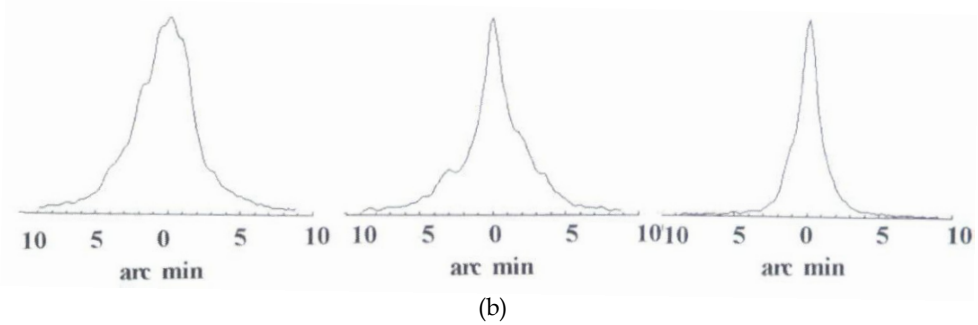

(b)

Fig. 18. Double-pass images for an eye with no lens, a soft contact lens and a rigid gas-permeable contact lens (a), and the corresponding intensity profiles as a function of the angle (b) (source: Torrents et al., 1997).

influence of ocular astigmatism on retinal image quality in this case (Torrents et al., 1997). In eyes with corneal astigmatism, the best results were obtained with rigid gas-permeable contact lenses because the lens offset the corneal astigmatism. The MTF was considerably smaller when no lenses or soft lenses were worn, even for small amounts of astigmatism (0.5 D) (Figure 18).

Finally, Vilaseca et al. (2009a) analysed the retinal image quality of eyes that had undergone kerato-refractive and phakic intraocular lens surgery by means of a double-pass system. In this study, residual astigmatism, and therefore retinal image quality, was found to be slightly different depending on the surgical procedure used. Although in general there was a high correction of astigmatism as well as good safety and efficacy indexes, some surgically induced astigmatism remained one month after surgery, especially in patients with intraocular lens implants.

5. References

Alió, J.L.; Schimchak, P.; Montés-Micó, R. & Galal A. (2005). Retinal image quality after microincision intraocular lens implantation. *J Cataract Refract Surg,* Vol. 31, No. 8 (August 2005), pp. 1557–1560.

Applegate, R.; Ballentine, C.; Gross, H.; Sarver, E. & Sarver, C. (2003). Visual acuity as a function of Zernike mode and level of root mean square error. *Optom Vis Sci,* Vol. 80, No. 2 (February 2010), pp. 97–105.

Atchison, D.A. & Smith, G. (2000). *Optics of the Human Eye* (1st edition), Butterworth-Heinemann, ISBN: 0-7506-3775-7, USA.

Atchison, D.A.; Guo, H.; Charman, W.N. & Fisher, S.W. (2009). Blur limits for defocus, astigmatism and trefoil. *Vision Res,* Vol. 49, No. 19 (September 2009), pp. 2393–2403.

Atkinson, J.; Braddick, O. & French, J. (1980). Infant astigmatism: its disappearance with age. *Vision Res*. Vol. 20, No. 11 (November 1980), pp. 891–893.

Artal, P.; Iglesias, I.; López, N. & Green, D.G. (1995a). Double-pass measurements of the retinal-image quality with unequal entrance and exit pupil sizes and the reversibility of the eye's optical system. *J Opt Soc Am A,* Vol. 12, No. 10 (October 1995), pp. 2358–2366.

Artal, P.; Marcos, S.; Navarro, R.; Miranda, I. & Ferro M. (1995b). Through focus image quality of eyes implanted with monofocal and multifocal intraocular lenses. *Opt Eng*, Vol. 34, No. 3 (March 1995), pp. 772–779.

Artal, P.; Berrio, E.; Guirao, A. & Piers, P. (2002). Contribution of the cornea and internal surfaces to the change of ocular aberrations with age. *J Opt Soc Am A Opt Image Sci Vis*, Vol. 19, No. 1 (January 2002), pp. 137–143.

Artola, A.; Patel, S.; Schimchak, P.; Ayala, M.J.; Ruiz-Moreno, J.M. & Alió, J.L. (2006). Evidence for delayed presbyopia after photorefractive keratectomy for myopia. *Ophthalmology*, Vol. 113, No. 5 (May 2006), pp. 735–741.

Baldwin, W.R. & Mills, D. (1981). A longitudinal study of corneal astigmatism and total astigmatism. *Am J Optom Physiol Opt*, Vol. 58, No. 3 (March 1981), pp. 206–211.

Bar-Sela, S.; Glovinsky, Y.; Wygnanski-Jaffe, T. & Spierer, A. (2009). The relationship between patient age and astigmatism magnitude after congenital cataract surgery. *Eur J Ophthalmol*, Vol. 19, No. 3 (March 2009), pp. 376–379.

Burton, G.J. & Haig, N.D. (1984). Effects of the Seidel aberrations on visual target discrimination. *J Opt Soc Am A,* Vol. 1, No. 4 (April 1984), pp. 373–385.

Campbell, F. W. & Green, D.G. (1965). Optical and retinal factors affecting visual resolution. *J Physiol*, Vol. 181, No. 3 (December 1965), pp. 576–593.

Charman, W.N. & Voisin, L. (1993a). Astigmatism, accommodation, the oblique effect and meridional amblyopia. *Ophthalmic Physiol Opt*, Vol. 13, No. 1 (January 1993), pp. 73–81.

Charman, W.N. & Voisin, L. (1993b). Optical aspects of tolerances to uncorrected ocular astigmatism. *Optom Vis Sci*, Vol. 70, No. 2 (February 1993), pp. 111–117.

de Gracia, P.; Dorronsoro, C.; Gambra, E.; Marin, G.; Hernández, M. & Marcos, S. (2010). Combining coma with astigmatism can improve retinal image over astigmatism alone. *Vision Res,* Vol. 50, No. 19 (September 2010), pp. 2008–2014.

de Vries, N.E.; Webers, C.A.; Tahzib, N.G.; Hendrikse, F. & Nuijts, R.M. (2008). Irregular astigmatism after cataract surgery resulting from inadequate clear corneal incision formation. *Cornea*, Vol. 27, No. 10 (March 2009), pp. 1176–1178.

Díaz-Doutón, F.; Benito, A.; Pujol, J.; Arjona, M.; Güell, J.L. & Artal, P. (2006). Comparison of the retinal image quality obtained with a Hartmann-Shack sensor and a double-pass instrument. *Invest Ophthalmol Vis Sci,* Vol. 47, No. 4 (April 2006), pp. 1710–1716.

Dougherty, P.J. & Bains, H.S. (2008). A retrospective comparison of LASIK outcomes for myopia and myopic astigmatism with conventional NIDEK versus wavefront-guided VISX and Alcon platforms. *J Refract Surg,* Vol. 24, No. 9 (November 2008), pp. 891–896.

Fernández-Vega, L.; Madrid-Costa, D.; Alfonso, J.F.; Montés-Micó, R. & Poo-López, A. (2009). Optical and visual performance of diffractive intraocular lens implantation after myopic laser in situ keratomileusis. *J Cataract Refract Surg,* Vol. 35, No. 5 (May 2009), pp. 825–832.

Güell, J.L.; Pujol, J.; Arjona, M.; Díaz-Doutón, F. & Artal, P. (2004). Optical quality analysis system: instrument for objective clinical evaluation of ocular optical quality. *J Cataract Refract Surg,* Vol. 30, No. 7 (July 2004), pp. 1598–1599.

Guirao, A.; Tejedor, J. & Artal, P. (2004). Corneal aberrations before and after small-incision cataract surgery. *Invest Ophthalmol Vis Sci*, Vol. 45, No. 12 (December 2004), pp. 4312–9.

Gwiazda, J.; Scheiman, M.; Mohindra, I. & Held, R. (1984). Astigmatism in children: changes in axis and amount from birth to six years. *Invest Ophthalmol Visual Sci*, Vol. 25, No. 1 (January 1984), pp. 88–92.

Haig, N.D. & Burton, G.J. (1987). Effects of wavefront aberration on visual instrument performance, and a consequential test technique. *Appl Opt*, Vol. 26, No. 3 (March 1987), pp. 492–500.

Harris, W.F. (1988). Algebra of sphero-cylinders and refractive errors, and their means, variance, and standard deviation. *Am J Optom Physiol Opt*, Vol. 65, No. 10 (October 1988), pp. 794–802.

Jiménez, J.R.; Ortiz, C.; Pérez-Ocón, F. & Jiménez, R. (2009). Optical image quality and visual performance for patients with keratitis. *Cornea,* Vol. 28, No. 7 (August 1987), pp. 783–788.

Keating, M.P. & Carroll, J.P. Blurred imagery and the cylinder sine-squared law. (1976). *Am J Optom Physiol Opt*, Vol. 53, No. 2 (February 1976), pp. 66–69.

Kragha, I.K. (1986). Corneal power and astigmatism. *Ann Ophthalmol*, Vol. 18, No. 1 (January 1986), pp. 35–37.

Legras, R.; Chateau, N. & Charman, W. N. (2004). Assessment of just-noticeable differences for refractive errors and spherical aberration using visual simulation. *Optom Vis Sci,* Vol. 81, No. 9 (September 2004), pp. 718–728.

Liang, J.; Grimm, B.; Goelz, S. & Bille, J.F. (1994). Objective measurement of the WA's aberration of the human eye with the use of a Hartmann-Shack sensor. *J Opt Soc Am A,* Vol. 11, No. 7 (July 1994), pp. 1949–1957.

McKendrick, A.M. & Brennan, N.A. (1996). Distribution of astigmatism in the adult population. *J Opt Soc Am A*, Vol. 13, No. 2 (February 1996), pp. 206–214.

Marcos, S.; Rosales, P.; Llorente, L. & Jiménez-Alfaro, I. (2007). Change in corneal aberrations after cataract surgery with 2 types of aspherical intraocular lenses. *J Cataract Refract Surg.,* Vol. 33, No. 2 (February 2007), pp. 217–226.

Mathur, A.; Atchison, D.A. & Charman W.N. (2009). Effect of accommodation on peripheral ocular aberrations. *J Vis,* Vol. 9, No. 12 (November 2009), pp. 20.1–11.

Millodot, M. & Thibault, C. (1985). Variation of astigmatism with accommodation and its relationship with dark focus. *Ophthalmic Physiol Opt*, Vol. 5, No. 3 (March 1985), pp. 297–301.

Montés-Micó, R.; Ferrer-Blasco, T.; Charman, W.N.; Cerviño, A.; Alfonso, J.F & Fernández-Vega, L. (2008). Optical quality of the eye after lens replacement with a pseudoaccommodating intraocular lens. *J Cataract Refract Surg*, Vol. 34, No. 5 (May 2008), pp. 763–768.

Navarro, R.; Santamaría, J. & Bescós, J. (1985). Accommodation-dependent model of the human eye with aspherics. *J Opt Soc Am A*, Vol. 2, No. 8 (August 1985), pp. 1273–1281.

Prieto, P.M.; Vargas-Martín F.; Goelz, S. & Artal, P. (2000). Analysis of the performance of the Hartmann-Shack sensor in the human eye. *J Opt Soc Am A,* Vol. 17, No. 8 (August 2000), pp. 1388–1398.

Pujol, J.; Arjona, M.; Arasa, J. & Badia, V. (1998). Influence of amount and changes in axis of astigmatism on retinal image quality. *J Opt Soc Am A,* Vol. 15, No. 9 (September 1998), pp. 2514–2521.

Raasch, T.W. (1995). Spherocylindrical refractive errors and visual acuity. *Optom Vis Sci,* Vol. 72, No. 4 (April 1995), pp. 272–275.

Radhakrishnan, H. & Charman, W.N. (2007). Changes in astigmatism with accommodation. *Ophthalmic Physiol Opt*, Vol. 27, No. 3 (May 2007), pp. 275–80.

Rabbets, R.B. (2007). *Clinical Visual Optics* (4th edition), Butterworth Heinemann Elsevier, ISBN-13: 978-0-7506-8874-1, USA.

Saad, A.; Saab, M. & Gatinel, D. (2010). Repeatability of measurements with a double-pass system. *J Cataract Refract Surg,* Vol. 36, No. 1 (January 2010), pp. 28–33.

Santamaría, J.; Artal, P. & Bescós, J. (1987). Determination of the point-spread function of human eyes using a hybrid optical-digital method. *J Opt Soc Am A,* Vol. 4, No. 6 (June 1987), pp. 1109–1114.

Saunders, H. (1986). Changes in the orientation of the axis of astigmatism associated with age. *Ophthalmic Physiol Opt*, Vol. 6, No. 3 (March 1986), pp. 343–344.

Saunders, H. (1988). Changes in the axis of astigmatism: a longitudinal study. *Ophthalmic Physiol Opt*, Vol. 8, No. 1 (January 1988), pp. 37–42.

Schallhorn, S.C.; Farjo, A.A.; Huang, D.; Boxer Wachler, B.S.; Trattler, W.B.; Tanzer, D.J.; Majmuder, P.A. & Sugar, A. (2008). Wavefront-guided LASIK for the correction of primary myopia and astigmatism. *Ophthalmology*, Vol. 115, No. 7, (July 2008), pp. 1249–1261.

Sloan, L.L. (1951). Measurement of visual acuity: a critical review. *Arch Ophthalmol*, Vol. 45, No. 6 (June 1951), pp. 704–725.

Tolhurst, D. J.; Tadmor, Y. & Chao, T. (1992). Amplitude spectra of natural images. *Ophthal Physiol Opt*, Vol. 12, No. 2 (April 1992), pp. 229–232.

Torrents, A.; Gispets, J. & Pujol J. (1997). Double-pass measurements of retinal image quality in monofocal contact lens wearers. *Ophthalmic Physiol Opt*, Vol. 17, No. 4 (July 1997), pp. 357–366.

Tunnacliffe, A.H. (2004). *Introduction to Visual Optics* (4th edition), TJ Reproductions, ISBN: 0-900099-28-3, England.

Ukai, K. & Ichihashi, Y. (1991). Changes in ocular astigmatism over the whole range of accommodation. *Optom Vision Sci*, Vol. 68, No. 10 (October 1991), pp. 813–818.

Vilaseca, M.; Padilla, A.; Pujol, J.; Ondategui, J.C.; Artal, P. & Güell, J.L. (2009a). Optical quality one month after Verisyse and Veriflex phakic IOP implantation and Zeiss MEL 80 LASIK for myopia from 5.00 to 16.50 diopters. *J Refract Surg,* Vol. 25, No. 8 (August 2009), pp. 689–698.

Vilaseca, M.; Arjona, M.; Pujol, J.; Issolio, L. & Güell J.L. (2009b). Optical quality of foldable monofocal intraocular lenses before and after injection: Comparative evaluation using a double-pass system. *J Cataract Refract Surg,* Vol. 35, No. 8 (August 2009), pp. 1415–1423.

Vilaseca, M.; Peris, E.; Pujol, J.; Borras, R. & Arjona, M. (2010a). Intra- and intersession repeatability of a double-pass instrument. *Optom Vis Sci,* Vol. 87, No. 9 (September 2010), pp. 675–681.

Vilaseca, M.; Padilla, A.; Ondategui, J.C.; Arjona, M.; Güell, J.L. & Pujol J. (2010b). Effect of laser in situ keratomileusis on vision analyzed using preoperative optical quality. *J Cataract Refract Surg*, Vol. 36, No. 11 (November 2010), pp. 1945–1953.

Wiggins, N.P. & Daum, K.M. (1991). Visual discomfort and astigmatic refractive errors in VDT use. *J Am Optom Assoc*, Vol. 62, No. 9 (September 1991), pp. 680–684.

Williams, D.R.; Brainard, D.H.; McMahon, M.J. & Navarro, R. (1994). Double-pass and interferometric measures of the optical quality of the eye. *J Opt Soc Am A,* Vol. 11, No. 12 (December 1994), pp. 3123–3135.

Williams, D.R.; Artal, P.; Navarro, S.; McMahon, M.J. & Brainard D.H. (1996). Off-axis optical quality and retinal sampling in the human eye. *Vision Res*, Vol. 36, No. 8 (April 1996), pp. 1103–1114.

Yao, K.; Tang, X. & Ye, P. (2006). Corneal astigmatism, high order aberrations, and optical quality after cataract surgery: microincision versus small incision. *J Refract Surg*, Vol. 22, No. 9, Suppl. (November 2006), pp. S1079–S1082.